TRANSMEMBRANE FLUX AND RECEPTOR DESENSITIZATION MEASURED WITH MEMBRANE VESICLES

Homogeneity of Vesicles Investigated by Computer Simulation

DEREK J. CASH, RICHARD M. LANGER, KATRAGADDA SUBBARAO, AND JULIE R. BRADBURY
Department of Biochemistry, University of Missouri-Columbia and Neurochemistry Unit, Missouri Institute of Psychiatry, St. Louis, Missouri 63139

ABSTRACT The use of membrane vesicles to make quantitative studies of transmembrane transport and exchange processes involves an assumption of homogeneity of the membrane vesicles. In studies of $^{86}Rb^+$ exchange mediated by acetylcholine receptor from the electric organ of *Electrophorus electricus* and of $^{36}Cl^-$ exchange mediated by GABA receptor from rat brain, measurements of ion exchange and receptor desensitization precisely followed first order kinetics in support of this assumption. In other measurements a biphasic decay of receptor activity was seen. To elucidate the molecular properties of receptors from such measurements it is important to appreciate what the requirements of vesicle monodispersity are for meaningful results and what the effect of vesicle heterogeneity would be. The experiments were simulated with single vesicle populations with variable defined size distributions as well as with mixtures of different populations of vesicles. The properties of the receptors and their density in the membrane could be varied. Different receptors could be present on the same or different membrane vesicles. The simulated measurements were not very sensitive to size dispersity. A very broad size distribution of a single vesicle population was necessary to give rise to detectable deviations from first order kinetics or errors in the determined kinetic constants. Errors could become significant with mixtures of different vesicle populations, where the dispersity in initial ion exchange rate constant, proportional to the receptor concentration per internal volume, became large. In this case the apparent rate of receptor desensitization would diverge in opposite directions from the input value when measured by two different methods, suggesting an experimental test for such kinetic heterogeneity. A biphasic decrease of receptor activity could not be attributed to vesicle heterogeneity and must be due to desensitization processes with different rates. Significant errors would not arise from the size dispersity apparent in subpopulations of vesicles seen by imaging techniques in membrane preparations.

INTRODUCTION

Since the recognition that sealed membrane vesicles are formed artifactually from membrane fragments broken off cells when they are disrupted, these native vesicles have been used as a tool to study transmembrane processes (Lehninger, 1964; Kasai and Clangeux, 1971; Racker, 1970; Kaback, 1970; Guidotti, 1979; Stein, 1986). The use of membrane vesicles allows the isolation of certain aspects of cellular machinery from the rest of the cell. For example a certain transport or channel protein may be located specifically on a particular vesicular membrane. The concentrations of solutions inside as well as outside the vesicle can be known and controlled, and the system can be manipulated and mixed as a suspension. Rapid mixing can be performed and measurements in short times can be made (Cash and Hess, 1981). Because of the relatively small size of vesicles, the surface-to-volume ratio is very much greater than that of a cell. A 20-μm-diameter neuron soma would have a surface-to-volume ratio 33-fold smaller than a 6,000-Å-diameter vesicle or 333-fold smaller than a 600-Å-diameter vesicle. This is of crucial significance with respect to the rates of surface-mediated changes of internal concentration. For example, the acetylcholine receptor mediated transmembrane equilibration of $^{86}Rb^+$ isotope tracer into vesicles formed from *Electrophorus electricus* electroplax is practically complete before the receptor is desensitized within ~300 ms, with a saturating concentration of acetylcholine, whereas the ion exchange occurring with a whole electroplaque cell before this desensitization of the receptor would be negligible.

Acetylcholine receptor–mediated $^{22}Na^+$ efflux from membrane vesicles was first demonstrated with a preparation from *E. electricus* (Kasai and Changeux, 1971). Subsequently the tracer ion efflux was shown to occur with first order kinetics in several minutes (Hess et al., 1975).

This efflux process is now known to have been due to the equilibrium concentration of open receptor channel after desensitization (Cash et al., 1985; Hess et al., 1983; Cash and Hess, 1980). It has since been shown that rapid receptor–mediated cation exchange occurs simultaneously with receptor desensitization in subsecond times (Hess et al., 1978; Hess et al., 1979) and that it is described by processes of ion-flux and receptor desensitization which are both kinetically first order (Cash and Hess, 1980; Cash et al., 1981). Similar results were observed with chloride ion exchange mediated by γ-aminobutyric acid (GABA) in membrane vesicles from rat brain. Rapid chloride exchange was shown to occur simultaneously with receptor desensitization, both processes apparently kinetically first order (Subbarao and Cash, 1985; Cash and Subbarao, 1987*a*). These observations of first order chemical kinetics were seen although the native membrane preparations used in these studies contained heterogeneous mixtures of membrane particles, as reviewed in the Discussion. On the other hand, in different experiments, curved concave first order plots have been reported which have been attributed to multiple phases of receptor desensitization each of which is kinetically first order (Cash and Subbarao, 1987*b–d*).

Because of the high specificity of these processes it is possible to make studies with relatively unpurified preparations of membrane. Indeed, when measurements reflecting the behavior of the membrane in vivo are desired, the minimum amount of purification manipulation may be preferred. The study of channel forming receptors by ion-flux measurements with vesicles may be useful with systems ranging from fresh native membrane preparations to cloned receptors in artificial lipid vesicles. It is important to consider to what extent these measurements reflect the size and size distribution of the vesicles on one hand and the molecular properties of the channel-forming proteins on the other.

The importance of the observation of discrete definable kinetic behavior of these processes is that it allows the meaningful expression of rates in terms of rate constants which can be compared with other measurements and with those predicted by hypothetical molecular mechanisms of the transport protein. Despite clear observations of precise first order kinetic behavior there has been some skepticism of the value of quantitative rate measurements with membrane preparations. Questions arise such as (*a*) what are the requirements for the observation of first order kinetics in terms of uniformity of the membrane vesicles or the singularity of the receptor? (*b*) Might a curved first order plot for desensitization reflect a dispersity of vesicle sizes rather than a multiplicity of receptor types?

In this paper we show examples in which first order desensitization of neurotransmitter receptors is demonstrated with high precision and examples which are not kinetically homogeneous. We describe a computer simulation of receptor mediated ion-exchange and receptor desensitization measured with vesicles, which allows the vesicle size distribution to be broad or heterogeneous and the receptors to be uniform or different. This simulation is used to investigate the effects of vesicle heterogeneity, or of a large breadth of size of a homogeneous population of vesicles, on the curve shapes or numerical values resulting from processes which are kinetically first order. The extent to which the nonlinear kinetics must be attributed to receptor multiplicity or vesicle dispersity is investigated. These considerations may be of interest not only for neurotransmitter receptors but for the analysis of transmembrane processes in general.

METHODS

Membrane Vesicle Preparations

Rat Cerebral Cortex. Male Sprague-Dawley rats, 4–6 wk old, were killed by decapitation. The cerebral cortex was rinsed with cold saline, cut into 1-mm slices and suspended in 30 ml solution A (0.32 M sucrose, 10 mM Hepes) (Calbiochem-Behring Corp., La Jolla, CA), pH 7.5, containing the protease inhibitors phenylmethylsulfonyl fluoride (1 mM), aprotinin (10 μg/ml), antipain (5 μg/ml), leupeptin (5 μg/ml), pepstatin A (5 μg/ml) (Sigma Chemical Co., St. Louis, MO), and the antioxidant, butylated hydroxytoluene (20 μM) at 0–4°C. The mixture was homogenized with a homogenizer (model 45, Virtis Co., Inc., Gardiner, NY) (setting 30) for 5 s. An equal volume of solution B (145 mM NaCl, 5 mM KCl, 1 mM $MgCl_2$, 1 mM $CaCl_2$, 10 mM glucose, 10 mM Hepes, pH 7.5) was added with gentle stirring and the mixture was centrifuged for 4 min, 270 *g*. The supernatant was centrifuged for 30 min, 23,640 *g*. The pellet was resuspended in 10 ml solution B, using a glass-Teflon hand homogenizer, diluted to 30 ml and centrifuged for 30 min, 23,640 *g*. The pellet was resuspended in 10 ml solution B and adjusted to 750 μg protein/ml. Protein concentration was assayed by the bicinchoninic acid method (Smith et al., 1985).

Electric Organ of E. electricus. The membrane vesicles (Kasai and Changeux, 1971) were prepared as described elsewhere (Fu et al., 1977; Sachs et al., 1982) with the modification that the homogenizing solution contained 1 mM phenylmethylsulfonyl fluoride, 3 mM sodium azide, 2 mM EGTA, 10 μM butylated hydroxytoluene, 1 mM $MgCl_2$, 3 mM Tris (hydroxymethyl) aminomethane (THAM), pH 7.5. Finally the vesicles were resuspended in solution C (169 mM NaCl, 5 mM KCl, 0.5 mM $CaCl_2$, 0.5 mM $MgCl_2$, 1 mM THAM, pH 7.5) and adjusted to 500 μg protein/ml for the experiment.

Receptor Desensitization The desensitization was followed by measuring the decrease in neurotransmitter-mediated isotope tracer influx into the vesicles due to preincubation of the membrane preparation with neurotransmitter for various times, using quench flow technique (Cash and Hess, 1981) as described previously (Aoshima et al., 1981; Cash and Subbarao, 1987*b*). The ion influx assays were initiated by the addition of solutions of acetylcholine or GABA containing the isotope tracer ions $^{86}Rb^+$ or $^{36}Cl^-$, respectively. The ion influx was terminated (quenched) by the rapid admixture of half the volume of *d*-tubocurarine (20 mM) or bicuculline methiodide (3 mM), respectively. These quenching procedures were shown to be complete and sufficiently rapid as reported elsewhere for the acetylcholine receptor (Cash and Hess, 1981; Hess et al., 1979) and the GABA receptor (Cash and Subbarao, 1987*a,d*). The concentrations of *d*-tubocurarine reported to be satisfactory for quenching the acetylcholine receptor for *E. electricus* were

~20-fold larger than those reported to be ineffective with the receptor from *Torpedo* species (Neubig and Cohen, 1980).

In the GABA experiments the ratio of signal to background varied in the region 1 to 2. The total counts were 200–300 cpm with a standard deviation typically of ±5 cpm. The standard deviation of GABA-mediated $^{36}Cl^-$ uptake is given by $\sigma = \sqrt{\sigma^2_{\text{background}} + \sigma^2_{\text{total}}}$, indicating that the signal-to-noise ratio is ~14 specific counts per σ and more than this in the acetylcholine experiments.

Treatment of Results. The transmembrane isotope exchange through the open channel form of a receptor, which is progressively attenuated by a desensitization process, is described by Eq. 1, where M_t/M_∞ is the fractional equilibration of isotope exchange in time t, and J and α are first order rate constants for ion-exchange and receptor desensitization, respectively. For a single phase of isotope exchange, Eq. 1 is fitted to the results to determine the values of J and α. The rate of desensitization, α, can be determined from the progress of ion flux when the isotope exchange rate is not fast enough to approach completion before desensitization and not slow enough to be terminated by desensitization before isotope exchange is significant. Outside these limits, the rate of desensitization can be measured by the preincubation technique.

$$\frac{M_t}{M_\infty} = 1 - \exp - J\left(\frac{1 - \exp - \alpha t}{\alpha}\right) \quad (1)$$

$$J = J_{(t_p=0)} \exp - \alpha_p t_p \quad (2)$$

$$-\ln\left(1 - \frac{M_t}{M_\infty}\right) = A \exp - \alpha_p t_p \quad (3)$$

$$A = J_{(t_p=0)}\left(\frac{1 - \exp - \alpha t}{\alpha}\right). \quad (4)$$

If the receptor is incubated for time t_p with neurotransmitter before the addition of the radioisotope tracer, the ion exchange activity (J) is decreased in the preincubation due to a reduction in the concentration of active receptor $[R']$ according to Eq. 2, where the subscript p refers to the preincubation. The decrease in isotope exchange (M_t/M_∞) in the assay (second) incubation is described by Eq. 3, which is derived from Eqs. 1 and 2, where A (Eq. 4) is a constant depending on the ion flux assay conditions. If the duration of the second (isotope exchange) incubation (t) is chosen so that the transmembrane equilibration of tracer ion is not complete, the decrease in receptor activity due to desensitization in the first incubation gives a decreased isotope exchange in the second incubation. Following Eq. 3, a plot of $\ln [-\ln (1 - M_t/M_\infty)]$ against preincubation time, t_p gives a diagnostic first order plot of ion exchange activity, the negative slope of which gives the rate constant for desensitization, α.

It should be noticed that measurements of initial rates of ion exchange in the second incubation are not required with this method of data treatment. The isotope exchange measured is an integrated function of the initial exchange rate and the desensitization rate (Eq. 1). The slope of the plot is independent of the conditions in the assay. The assay conditions control the value of the ordinate intercept, A (Eq. 4). Conditions are chosen to give a significant fraction of the equilibrium value of isotope exchange. The validity of this treatment is not limited by the presence of a very high number of receptors.

In contrast, the assumption that linear, initial rates of ion flux are measured in a constant assay time can be valid only within a limited range of rates. With that approximation the measurement must be made before the rate is depleted, by the decreasing concentration gradient or by desensitization. The measurement must be restricted to a small fraction of the equilibrium value of isotope exchange. Factors increasing the ion exchange rate may place the measurement outside the valid range unless a reduction of assay time is made within the series of experiments. A method of data treatment based on this approximation could be used only with the appropriate assay conditions for a limited range of rates.

TABLE I
PARAMETERS USED IN THE EQUATIONS

M_t/M_∞	Fractional equilibration of receptor mediated ion flux at time t
α	First order rate constant for desensitization
J	Initial first order rate constant for ion flux
$[R']$	Receptor concentration per internal volume
SA	Surface area
V	Internal volume
r	Vesicle radius
Subscripts	
i	In the ith element
p	In the preincubation (in the absence of subscript p the parameter pertains to an incubation containing tracer radioisotope)
$(t_p = 0)$	Value with no preincubation

Computer Simulation

The Vesicle Populations. Each different population of vesicles can be defined in terms of either surface area (SA) or internal volume (V) or receptor concentration on the vesicle membrane per internal volume ($[R']$). The distribution of each of these properties may be described by a normal, Poisson, or binomial distribution. The receptor on the vesicles is defined in terms of its two dimensional concentration on the membrane, its desensitization rate constant, α, and its rate constant for ion translocation through the open channel, $\bar{J}$. The fraction of the receptor in the open channel states, $\bar{A}$, can be input directly or calculated assuming a particular mechanism from the appropriate equations and the ligand concentration. The simulations can be made with single populations of vesicles of various breadths and shapes and also with mixtures of two different vesicle populations in any proportion. A single population of vesicles can contain two different types of receptor. Different vesicle populations in a mixture can contain the same or different receptors. With these simulated vesicle suspensions, measurements of ion flux and receptor desensitization can be computed. The inputs for the properties of the vesicles and the receptors are summarized in Appendices A and B, respectively.

The size distributions of the vesicle populations were divided into 21 narrow elements. These are positioned about a center point to cover the distribution of each population. The percentage of the area under the distribution curve covered by the elements is displayed so that it can be confirmed that the elements cover the distribution curve. Distribution curves characterizing the vesicle populations in various ways can be displayed (Appendix C). The properties of each element are displayed in the spreadsheet (Appendix D). These include the fraction of vesicles in the element, their surface area, internal volume, and the value of J. It was shown that the same result was obtained when 41 elements were taken from each population.

Isotope Exchange. The initial rate constant for ion exchange into a vesicle varies according to Eq. 5 where $\bar{A}$, $[R']$, and $\bar{J}$ are as defined above (Hess et al., 1980, 1981). The vesicles in each element were assumed to be uniform and spherical. Each receptor was assumed to desensitize completely in a single exponential phase. The fractional

equilibration of the ion exchange $(M_t/M_\infty)_i$ in a monodisperse element i is given by Eq. 6 where t is the reaction time, and J_i and α are the rate constants for ion flux and desensitization, respectively.

$$J_i = \bar{J}\bar{A}[R']_i \tag{5}$$

$$\left(\frac{M_t}{M_\infty}\right)_i = 1 - \exp - J_i\left(\frac{1 - \exp - \alpha t}{\alpha}\right) \tag{6}$$

$$\frac{M_t}{M_\infty} = \sum_i \left[\left(\frac{M_t}{M_\infty}\right)_i \frac{V_i}{V}\right]. \tag{7}$$

The uptake of tracer ion into each element was calculated with Eq. 6. The ion flux for the whole population was obtained by summing that in each element in proportion to the partial internal volume of the elements (Eq. 7). The total specific internal volume $V(=\Sigma_i V_i)$ is the sum of the internal volumes in the elements, V_i. The same procedure was followed where the mixture of vesicles contained more than one population. The effect of heterogeneity of the vesicles or receptor on the measurements of the receptor-mediated ion influx at various times can be seen by comparing the values of M_t/M_∞ calculated from Eq. 7 with those calculated from Eq. 1 assuming a homogeneous vesicle population.

Desensitization. Measurements of receptor desensitization were simulated in the same way. The effect of heterogeneity of the vesicles or receptor on the measurements of desensitization can be seen by comparing the results plotted according to Eq. 3 using simulated values of M_t/M_∞ calculated from Eq. 7 with those calculated using the values of M_t/M_∞ calculated directly from Eq. 1 assuming homogeneous vesicles and receptor.

RESULTS

Experimental Measurements

The acetylcholine mediated desensitization of acetylcholine receptor from the electric organ of the eel, *E. electricus*, with high (1,000 μM) and low (30 μM) acetylcholine concentrations is shown in Fig. 1. The desensitization is shown to follow first order kinetics, with greater precision than in previous reports, over the loss of at least ~80% of the activity.

The GABA-mediated desensitization of GABA receptor from rat cerebral cortex also followed first order kinetics as shown with high (500 μM) and low (10 μM) GABA concentrations in Fig. 2, *a* and *b*. This first order behavior was seen with a small proportion of the membrane preparations (Cash and Subbarao, 1987*a*,*b*) over a loss of at least 80–90% of the activity. Other preparations lost chloride exchange activity in a way giving a nonlinear first order plot as illustrated in Fig. 2*c* for two concentrations of GABA. This could be fitted to a biphasic decay of activity (Cash and Subbarao, 1987*b*,*c*).

General Description of Computer Simulations

The vesicle population, defined in one of several ways (see Methods), is split into the 21 elements for the computation as indicated in Fig. 3. For the same vesicles the distribution of vesicle volumes ($V\alpha r^3$) (r = vesicle radius) is broader than that of surface area ($SA\alpha r^2$) and the distribution of

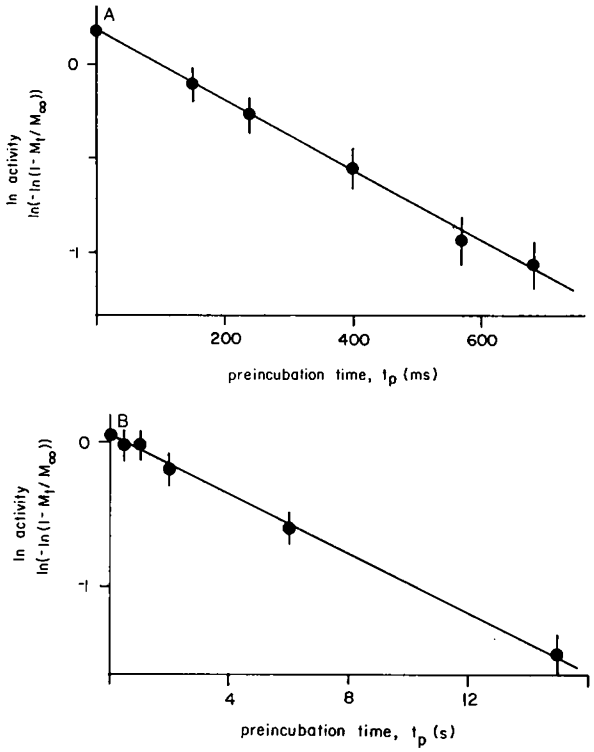

FIGURE 1. Desensitization of acetylcholine receptor by its exposure to acetylcholine. Experimental data is fitted to a first order kinetic plot calculated from Eq. 3. The rate constant for desensitization is given by the negative slope of the line. (*A*) Desensitization with 1,000 μM acetylcholine. The $^{86}Rb^+$ influx was assayed with 1,000 μM acetylcholine for 1.0 s. The rate constant for desensitization was 5.1 s^{-1}. (*B*) Desensitization with 30 μM acetylcholine. The $^{86}Rb^+$ influx was assayed with 1,000 μM acetylcholine for 1.0 s. The rate constant for desensitization was 0.85 s^{-1}. The quench flow method was the same as described in the legend to Fig. 2, but the reaction was in solution C, 1°, pH 8.0, containing acetylcholine. The quench reagent was *d*-tubocurarine (20 mM) in solution C.

receptor concentration per internal volume ($[R']\alpha\ 1/r$) is much narrower, approaching a monodisperse population. It is the uniformity of this receptor concentration $[R']$ that is relevant to the uniformity of the initial ion exchange rate (Eq. 5). The initial ion exchange rate constant, J, is the volume average of the values for each uniform element, for any breadth of distribution or mixture of populations, and this can be calculated from the $[R']$ value for the whole population.

$$J = \bar{J}\bar{A}[R'] = \bar{J}\bar{A}\sum_i \left([R']_i \frac{V_i}{V}\right) = \sum_i \left(J_i \frac{V_i}{V}\right). \tag{8}$$

Measurements of the time course of ion exchange into the vesicles and of the desensitization of the receptor were simulated by summing the computations of ion exchange for the uniform elements. These results were compared with those calculated assuming a monodisperse population. For example, the population of membrane vesicles which is described by the distribution curves in Fig. 3 was defined as having a normal distribution of internal volume with a center volume of 2.4×10^{-11} μl per vesicle and a breadth

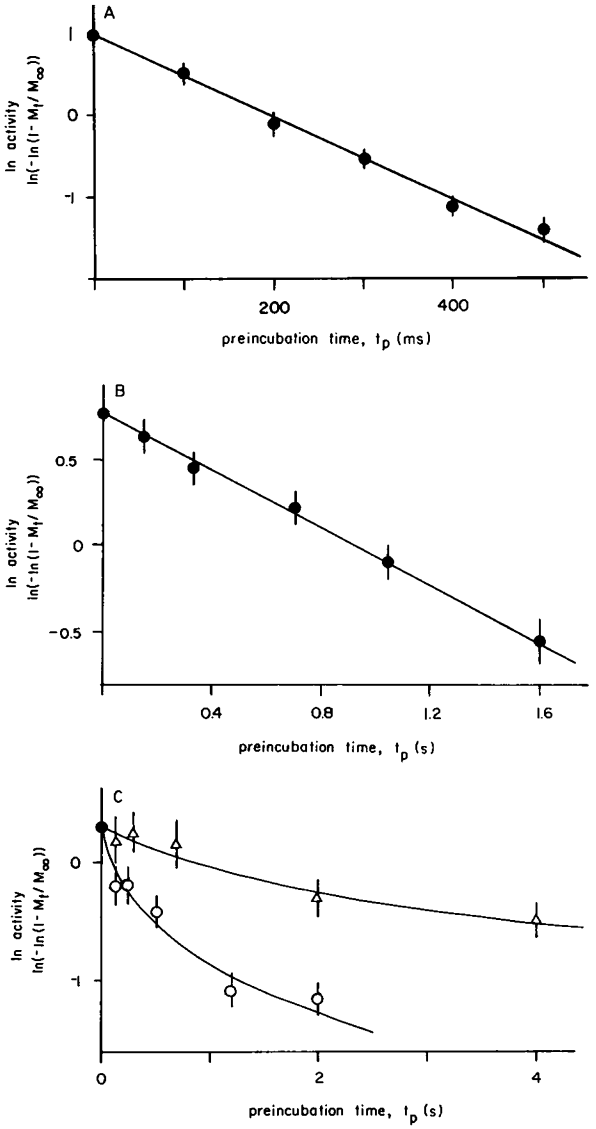

FIGURE 2 Desensitization of GABA receptor by its exposure to GABA. Examples of first order and biphasic desensitization of GABA receptor. (*A*) Desensitization with 500 μM GABA. The chloride influx was assayed with 10 mM GABA for 320 ms. The rate constant for desensitization was 1.8 s^{-1}. (*B*) Desensitization with 10 μM GABA. The chloride influx was assayed with 1 mM GABA for 320 ms. The rate constant for desensitization was 0.10 s^{-1}. The reproducibility of the determinations was ±6 cpm (SD), 6%. The experimental data is fitted to a first order kinetic plot according to Eq. 3. The rate constant for desensitization is given by the negative slope of the line. (*C*) Biphasic desensitization. Measurements with the same membrane preparation with (△) 20 μM GABA and (○) 100 μM GABA. The zero preincubation time, t_p points (●), determined with no GABA in the preincubation, were shown to be independent of t_p and correspond to no desensitization in the preincubation. The lines were computed assuming two different receptors with different rates of desensitization on the same vesicle population. The rates of desensitization were (*A*) $\alpha = 0.8\ s^{-1}$, $\beta = 0.08\ s^{-1}$ and (*B*) $\alpha = 6.0\ s^{-1}$, $\beta = 0.6\ s^{-1}$. The $^{36}Cl^-$ influx assay was with 500 μM GABA. The reproducibility of the determination was ±8% (SD) of the initial signal. The reaction was measured in solution B at 30°. The vesicle preparation (225 μl) in solution B was mixed with solution B, pH 7.5, containing GABA (225 μl). After the time on the abscissa, the mixture was mixed with solution B containing $^{36}Cl^{-1}$ (20 μCi/ml) and GABA (30 mM) (225 μl). After 320 ms the second incubation mixture was mixed with

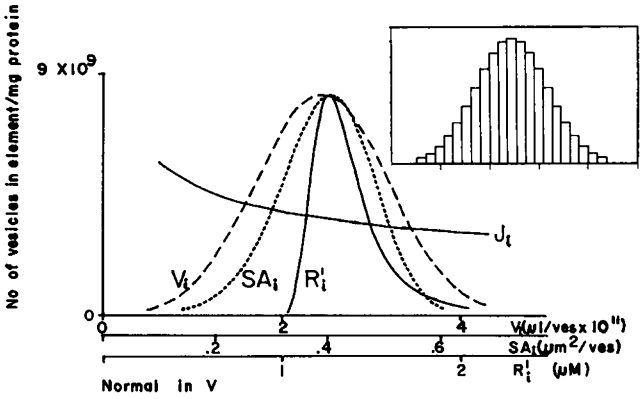

FIGURE 3 A hypothetical population of vesicles defined as having a normal distribution of internal volume with a center diameter of 3,600 Å and a single type of receptor with a uniform density on the surface of 46/μm^2. The vesicles are described in terms of distribution curves with respect to internal volume (V), surface area (SA), and receptor concentration per internal volume [R']. The ion flux rate (J_i), for the different vesicle sizes shown on the V_i scale, decreased from 27 s^{-1} in the first element to 14 s^{-1} in the 21st element, these values corresponding to $J = 16.8\ s^{-1}$ for the whole population. This assumes constant receptor density on the membrane. (*Inset*) The distribution, in terms of internal volume, is divided into 21 elements for individual computations of ion flux.

given by the standard deviation, σ, of 30% of that volume. To investigate a large dispersity of vesicles, a mixture of two populations of different sizes could be simulated (e.g., Fig. 4). To investigate the effect of multiplicity of receptors, different receptors could be put on a single vesicle population, or a mixture of two populations of vesicles each with a different receptor could be simulated.

Distribution of Receptor Concentration [R']

The dispersity of vesicle size and receptor density were varied systematically with single and mixed populations of vesicles while keeping the properties of the receptor constant. It was found that insofar as the receptor concentration per internal volume [R'] was made disperse, a discrepancy was introduced between the simulated results and those calculated for a monodisperse value of [R']. This is illustrated by the mixture of vesicles described in Fig. 4. With this relatively wide dispersity of [R'] the discrepancy reaches a magnitude that would be detectable with our experimental precision. The simulated ion exchange

bicuculline methiodide (3,000 μM) in solution B and passed through a glass fiber filter disc (Whatman GF/C). The membrane retained on the filter was washed with solution B (3 × 10 ml), dried, and counted with scintillation fluid. In a control experiment to check vesicle integrity, GABA was omitted from the first incubation at the shortest and longest first incubation times. M_∞ was determined by omitting GABA from the first incubation and extending the second incubation time to 6 s. The unspecific flux baseline was determined by omitting GABA from both incubations (Cash and Subbarao, 1987*b*). The initial specific ion flux count was 109 cpm on a background of 95 cpm. Each determination was done in triplicate.

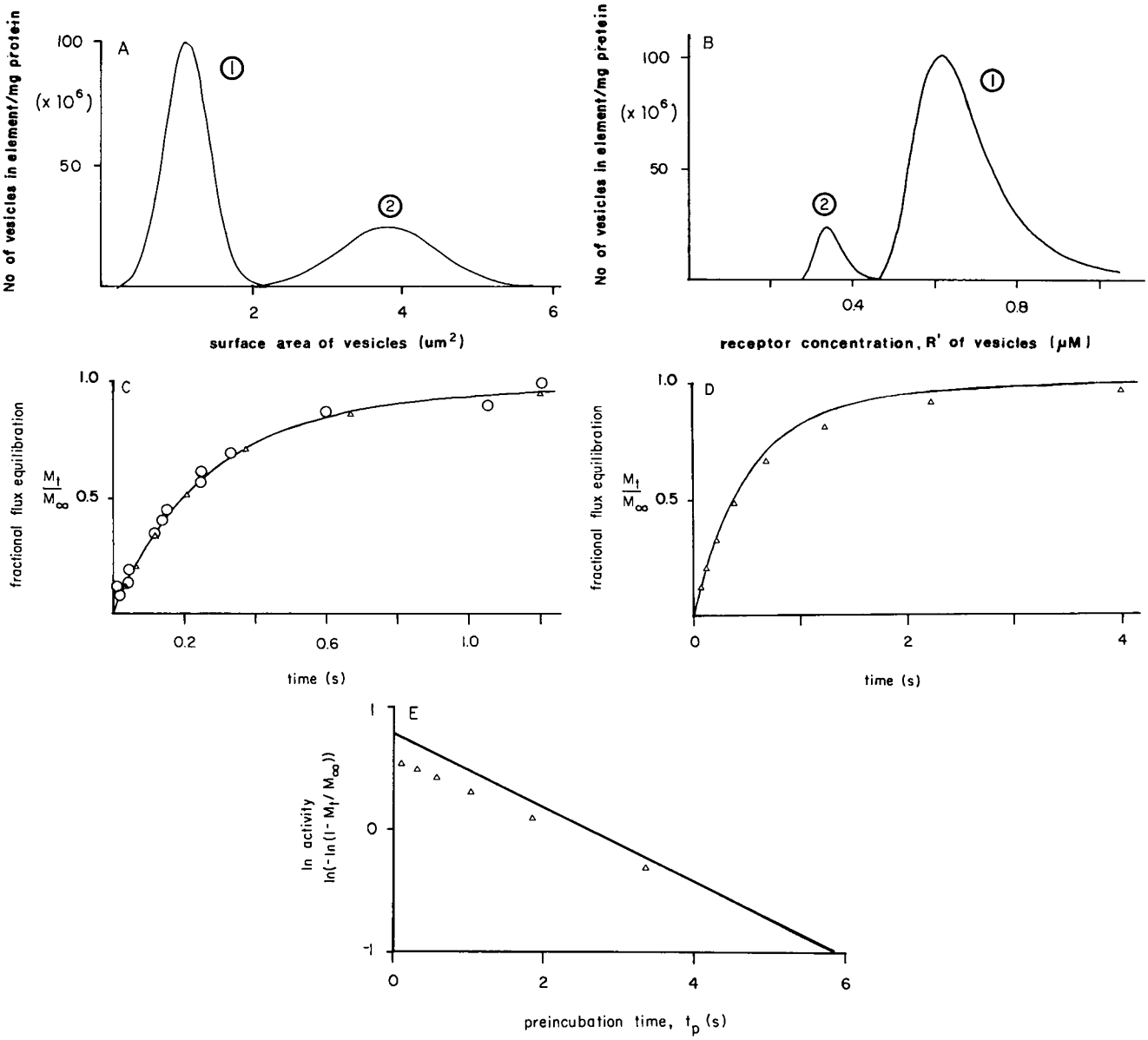

FIGURE 4 Two vesicle populations with the same membrane defined as having normal distributions of surface area with central diameters of (*i*) 6,000 Å and (*ii*) 11,000 Å. A single type of receptor is present with a uniform density of 36.9/μm^2. The internal volumes of each population are equal. (*A*) The distribution curves of surface area (*SA*). (*B*) The distribution curves of receptor concentration per internal volume ([*R'*]). The larger vesicle population has the smaller *R'* and hence *J*. (*C*) Simulation of ion flux for the larger sized population only (△) (Eqs. 6 and 7) compared with the line calculated assuming monodisperse vesicles (Eq. 1) and with experimental measurements (O) of the GABA receptor–mediated chloride influx with 40 μM GABA (Cash and Subbarao, 1987*a*). The experimental reproducibility was ±5% of the maximal signal. The experimental points are means of triplicates. The values used in the calculations were $J = 3.8\ s^{-1}$, $\alpha = 0.7\ s^{-1}$ (*D*) Simulation of ion flux for the mixture of both populations. The points show the simulated ion flux (Eq. 7). The line is calculated assuming monodisperse vesicles (Eq. 1). The values are $J = 1.96\ s^{-1}$, $\alpha = 0.3\ s^{-1}$. A calculated line to best fit the simulated results would have a value for α increased by up to a factor of 2 (J kept constant). The discrepancy is larger than the experimental error of the measurements. (*E*). Simulation of the measurement of desensitization (Eq. 3). The points are simulated by summing M_t/M_∞ in the elements (Eqs. 6 and 7). The line is calculated assuming monodisperse vesicles (Eq. 1). The value of α was $0.3\ s^{-1}$ (assay conditions $J = 8.3\ s^{-1}$, $\alpha = 1.3\ s^{-1}$). The value which would fit the simulation was $\alpha = 0.26\ s^{-1}$ (with $J = 8.3\ s^{-1}$). This discrepancy is larger than the experimental error of the measurements.

(M_t/M_∞) is always lower than that calculated for a monodisperse [*R'*]. The deviation of the simulations increases with the amount of ion exchange giving rise to sharper curves for the time course of ion flux (e.g., Fig. 4 *d*, points) and convex curves for the preincubation experiments (e.g., Fig. 4 *e*, points) with slopes lower than the continuous line calculated for a monodisperse [*R'*]. These distortions are the same shapes, whatever the origin of the dispersion of the [*R'*] values (vesicle size dispersity, receptor density dispersity, etc.). This discrepancy would give rise to an

error in the determination of α by curve fitting if homogeneity was assumed. But this error would be in opposite directions for the two methods. The curve shapes are distorted so that the apparent desensitization rate α would be higher than the real (input) value when determined by fitting Eq. 1 to the time course of ion exchange (Fig. 4 *d*) but lower than the real (input) value when determined by fitting Eq. 3 to the preincubation experiments (Fig. 4 *e*). The value of the initial rate constant for ion exchange J, which would be obtained fitting Eq. 1 to the progress of ion exchange, is a volume averaged mean (Eq. 8). In practice, making the best fit of Eq. 1 to the experimental points over the whole curve rather than to the initial rate would give a J value slightly lower than this, with the increased α value, if the shape was distorted due to heterogeneity.

For each of the individual populations illustrated, the effect of the vesicle dispersity on the measurements of isotope exchange or receptor desensitization would not be detectable. This is illustrated for the larger (lower $[R']$ and slower ion exchanging) population in Fig. 4 *c*, in which are shown also some typical measurements of GABA receptor mediated ion influx. Similarly for the population described in Fig. 3, the distortion of the measurements due to the dispersity of vesicles would be less than the experimental error because the dispersity of ion exchange rates (J α $[R']$) is relatively narrow.

In another simulation, a mixture of two vesicle populations made of the same membrane, of mean diameter 3,600 and 7,000 Å and equal total internal volume, had initial ion flux rate constants of $J = 13.5\ s^{-1}$ and $J = 6.9\ s^{-1}$, respectively, and a receptor desensitization rate constant of $4.0\ s^{-1}$. Simulated experiments gave values of $J = 10.2\ s^{-1}$ and $\alpha = 4.6\ s^{-1}$ by fitting Eq. 4 to the time course of ion-flux and $\alpha = 3.6\ s^{-1}$ by fitting Eq. 6 to the decrease of ion flux in the preincubation experiment. The real dispersity of J values gave rise to a discrepancy in the measured values.

Distribution of Ion Translocation Rate per Receptor

Other factors that increase the distribution of the values of the ion exchange rate constant J (Eqs. 5 and 8) give rise to the same deviations from homogeneous kinetics as those described above due to dispersity of receptor concentration $[R']$. These properties are the specific rate for ion translocation, $\bar{J}$, and the fraction of the channel in the open state, $\bar{A}$, which is controlled by a number of factors. These include the ligand dissociation constant, the channel opening equilibrium, and the fraction of the receptor which is active (not desensitized or inhibited). Increasing the dispersity of these properties of the receptor gave rise to the deviations described above. However these effects of dispersity of ion exchange rate appeared only when the different receptors were concentrated on different vesicle populations. If the different receptors were distributed over the vesicles in the same proportions, the ion-exchange rates would be averaged on the vesicles and would not give rise to the deviations discussed.

Distribution of Rate of Desensitization

When receptors with different rates of desensitization were introduced, the loss of activity due to desensitization was described by a concave curve as illustrated by the calculated lines in Fig. 2 *c*. Thus dispersity of desensitization rates gives a deviation from linearity with the opposite curvature to that caused by dispersity of ion exchange rate. A concave shape appears whether or not the different receptors are on different membrane vesicles. When the different receptors are on different vesicles, the semilog plots of activity loss are not theoretically sound as diagnostic first order plots. However, in this case also, the observation of concave curvature would indicate the presence of receptors that are desensitized with different rates.

Distribution of Vesicle Size

A range of vesicle sizes would contribute to a deviation from homogeneous kinetics insofar as it caused a dispersity in receptor concentration per internal volume $[R']$. $[R']$ increases with decreasing vesicle size, reflecting the changing surface/volume ratio, in a way depending on the assumptions of receptor density. For a given membrane receptor density $[R']$ α $1/r$, (r = vesicle radius) or for a given total number of receptors $[R']$ α $1/r^3$. For example, the nonhomogeneous kinetics reflecting the heterogeneous vesicles described in Fig. 4 result from dispersity of vesicle size. A single receptor with a uniform density on the membrane is present throughout.

DISCUSSION

The computer simulations showed that the observation of first order kinetics for the progress of receptor-mediated ion exchange and desensitization requires homogeneity of the vesicles and the receptor. Thus a broad dispersity of vesicle sizes could cause a distortion in the observation of the kinetic properties of a receptor (e.g., Fig. 4, *d* and *e*). However, the measurements are rather insensitive to such dispersity, and a very broad distribution of $[R']$ ($\sigma > 25\%$ of the mean value for a single normal distribution in $[R']$) would be required to give significant errors. Errors due to the breadth of the single populations in the examples given were not significant. Therefore mixtures of different vesicle populations were simulated to illustrate the introduction of discrepancies larger than experimental error. If an error due to vesicle heterogeneity were to exist, the rate of desensitization estimated from the progress of ion exchange (Fig. 4 *d*) would be increased, whereas that estimated from the decrease of ion exchange due to preincubation (Fig. 4 *e*) would be decreased. This divergence of result between the two methods would be diagnostic of errors due to vesicle heterogeneity. Such a divergency has not been observed experimentally in studies with

acetylcholine receptor and GABA receptor so far. Therefore, it seems unlikely that there are errors due to a broad size distribution of vesicles or the existence of receptors on different sized vesicle populations in the systems which have been studied in detail.

Specifically, the monodispersity required is of the ion exchange rate constant J of the vesicles, which is a property of the vesicles and depends on the nature of the receptor and its concentration per internal volume $[R']$ (Eq. 5). The origin of the discrepancy when homogeneity does not exist is the summing of differently shaped ion exchange curves corresponding to different values of J. This causes a convex semilog plot of receptor activity (e.g., Fig. 4, points). The discrepancy increases with the fractional ion exchange, M_t/M_∞. This vesicle inhomogeneity might arise from dispersity of $[R']$, for example, due to dispersity of vesicle size or shape or receptor density.

Multiplicity of receptor type could contribute to nonlinear semilog plots of activity in two ways. Firstly, differences in receptors on different vesicles could cause a dispersity of the factors controlling rate of chloride exchange and hence J (Eq. 5). The effect would be equivalent to the vesicle heterogeneity discussed above. Secondly, differences in desensitization rates of the receptors would give rise to a concave semilog plot (e.g., Fig. 2 *c*). Because such a deviation could not be caused by vesicle heterogeneity, its observation must be attributed to different phases of desensitization. Whether these are due to a single receptor or to different receptors can be determined by examining the effect of varying neurotransmitter concentration on the ordinate intercept of this plot (Cash and Subbarao, 1987*b*). Similar receptors with different ion translocation rates would be detected in these experiments only when they have different desensitization rates or when they give rise to dispersity of ion translocation rate constants due to their uneven distribution over the vesicles.

Membrane preparations prepared from *E. electricus* which contained vesicles with active acetylcholine receptor (Kasai and Changeux, 1971) also contained other types of membrane vesicle (Bauman et al., 1970; Cartaud et al., 1971; Hess et al., 1975). Relatively impermeable vesicles containing the receptor could be enriched on the basis of their permeability on a sucrose density gradient (Rosenberg et al., 1977). The volume accessed via the acetylcholine receptor was ~20% of the total internal volume (Hess et al., 1975). Further purification of these vesicles was based on their permeability to cesium ion on a cesium chloride gradient (Hess and Andrews, 1977). The "active" vesicles purified on a Percoll gradient in the presence of CsCl (Sachs et al., 1982) appeared relatively homogeneous in size, compared with the unfractionated mixture, having a diameter of 3,600 ± 600 Å (Hess et al., 1983). Although the measurements of ion flux and receptor desensitization were normally made with the unfractionated vesicle suspension, the results reflect the active vesicle population. The precise first order kinetics of the desensitization of the acetylcholine receptor shown in Fig. 1 supports the previous observations of the first order desensitization and ion flux processes (Cash and Hess, 1980; Cash et al., 1981; Aoshima et al., 1981) and also of the slow first order ion flux process, due to receptor remaining after the rapid desensitization, with unfractionated (Hess et al., 1975) as well as purified (Hess and Andrews, 1977) vesicles. A fast phase of desensitization of cation flux mediated by acetylcholine receptor from *Torpedo californica* was also reported to follow first order kinetics (Walker et al., 1981; Hess et al., 1982). The lack of deviation from first order kinetics is consistent with a single receptor type and a vesicle population with a relatively narrow range of receptor concentration per internal volume $[R']$ consistent with the relatively narrow size dispersion.

Membrane preparations prepared from *Torpedo sp.* also contained a heterogeneous mixture of vesicles (Cartaud et al., 1978; Strader et al., 1979). In this case a larger internal volume (~70%) was accessed by the acetylcholine receptor channel (Jeng et al., 1981). The active fraction could be enriched by velocity centrifugation in a sucrose gradient, and contained a relatively narrow size distribution of vesicles (Jeng et al., 1981).

In membrane preparations from mammalian brain, synaptosomes, derived from the presynaptic membrane, are the major vesicular component (Gray and Whittaker, 1962; DeRobertis et al., 1962). Several modifications of the "synaptosome" preparation have been made after homogenization in sucrose solution (Cotman and Mathews, 1971; Sun and Sun, 1972; Hajos, 1975; Booth and Clark, 1978; Dodd et al., 1981; Loescher et al., 1985). In electron micrographs the membrane appears to be heterogeneous. In differential centrifugation studies a "synaptosome" preparation showed characteristics of heterogeneously dispersed particles (Cotman et al., 1970). However the particles identifiable as synaptosomes appeared to be relatively uniform in size.

Membrane preparations prepared after gentle homogenization in buffered salt solutions are reportedly somewhat different (Hollingsworth et al., 1985; Daly et al., 1980; Chasin et al., 1974), although they also appear to be heterogeneous. Several types of vesicular structure are discernible (Psychoyos et al., 1982; Horn and Phillipson, 1976) including synaptosomes and neurosomes, the latter believed to be derived from the postsynaptic membrane and synaptoneurosomes believed to be these two vesicles joined by the synaptic structure (Hollingsworth et al., 1985). Different populations of vesicles, including synaptosomes and neurosomes in the heterogeneous mixture, each appeared to be spherical and monodisperse in size on examination with light microscopy (Hollingsworth et al., 1985) and also by scanning electron microscopy (Psychoyos et al., 1982), suggesting that the deformed spheri-

cal shape of membrane vesicles sometimes seen with transmission electron microscopy may result from the sample preparation procedures.

Transmembrane chloride flux mediated by GABA has been reported with preparations from sucrose solution homogenates (Sanchez et al., 1984; Subbarao and Cash, 1985; Cash and Subbarao, 1987*a–d*) as well as homogenates made in buffered salt solutions (Harris and Allan, 1985; Schwartz et al., 1986). The volume accessed specifically via the GABA receptor is small (Cash and Subbarao, 1987*a*), giving rise to $^{36}Cl^-$ exchange with only 6.5–13% of the total exchangeable chloride. So it is difficult at this stage to assign the vesicles containing active GABA receptor to particular populations seen by the imaging techniques. The first order kinetics of the loss of activity during desensitization of GABA receptor shown in Fig. 2, *a* and *b* supports the operation of a single type of receptor or different receptors which desensitize with similar rates on a vesicle population that is kinetically homogeneous. These results support the previous observation of a first order chloride flux process progressively attenuated by a first order GABA receptor desensitization process (Cash and Subbarao, 1987*a*; Subbarao and Cash, 1985). They are consistent with the presence of active GABA receptor on a minor vesicular component, in the membrane suspension, which does not have a very broad distribution of receptor concentration per internal volume [R'].

Biphasic first order plots of desensitization of the GABA receptor have been generally seen (e.g., Fig. 2 *c*) (Cash and Subbarao, 1987*b*,*c*) although a single phase has sometimes been observed and can be ensured by removal of the faster phase by preincubation with GABA (Cash and Subbarao, 1987*a*). The computer simulations showed that this concave curve shape cannot be caused by a heterogeneous or broadly dispersed mixture of vesicles and that its explanation requires receptors with different rates of desensitization. This conclusion is supported by the long regions of linear (first order) decay of activity which can be observed in these biphasic preparations in appropriate conditions (Cash and Subbarao, 1987*b*).

The homogeneous kinetics observed with the acetylcholine receptor and the GABA receptor with membrane preparations from tissue homogenates support the existence of specific vesicle populations with size distributions that are not too broad. This is consistent with the appearance in the preparations of particular vesicle populations with relatively narrow size distributions. Apparently a particular type of membrane will form vesicles of a characteristic, particular size. On this basis one might generally expect to observe homogeneous kinetics from channel forming neurotransmitter receptors, and other transport mechanisms in membrane preparations, and that deviations from simple kinetics usually reflect differences in the nature of the transport proteins themselves. Where this is not the case, inaccuracies caused by a nonuniform receptor concentration per internal volume [R'], whatever the origin of this, can be exposed by the diverging values of desensitization rate measured by the two different types of experiment described.

APPENDIX

A. Inputs of Vesicle Properties

1. Parameters describing width, skew, and center diameter for the distribution equation being used (normal, Poisson, or binomial).
2. Receptor concentration R (pmol/mg total protein, with total protein meaning the total membrane protein in the whole distribution).
3. Internal volume V (μl/mg total protein). In a series of simulations, in which the quantity of membrane remains constant, when there is a change of vesicle size, V can be either kept constant or allowed to vary so that the receptor density (No. of receptors/μm^2) remains constant.
4. Where two populations are mixed, a percent of the internal volume for each is specified.
5. At this stage various properties of the vesicle population are displayed including:
No. of receptors per mg total protein
Mean No. of receptors per vesicle
Concentration of receptors per internal volume (μM)
mg protein per μm^2
No. of receptors/μm^2
Center volume (μl)
Center surface area
Center R' (μM)
No. of vesicles/mg total protein.
6. The percentage of the area under the distribution curve covered by the elements is displayed. This is adjusted to ≃99% by adjusting the width of the elements.

B. Inputs of Receptor Properties

1. The initial rate constant for ion flux, J, and the rate constant for desensitization, α.
2. Alternatively the value of J was computed from $\bar{J}$ and $\bar{A}$. $\bar{A}$ was computed from the parameters of the receptor pertaining to the appropriate model.

C. Display of Distributions and Properties of Vesicles in the Elements

The following distribution curves can be displayed.
1. No. of vesicles in the element per mg total protein/surface area
2. No. of vesicles in the element per mg total protein/[R'] in the element
3. No. of vesicles in the element/internal volume of vesicles in the element
4. Internal volume in the element (μl/mg total protein)/surface area of vesicles
5. Internal volume in the element/[R'] in the element.

D. Calculated Properties of Receptor-Containing Vesicles in Each Element

The following properties of the vesicles in each element are tabulated on the spreadsheet.
1. Fraction of vesicles in the element
2. Surface area of the vesicles
3. Internal volume of the vesicles
4. No. of receptors/vesicle
5. No. of vesicles/mg total protein

6. Internal volume/mg total protein
7. Surface area in the element/mg total protein
8. No. of receptors in the element/mg protein
9. Concentration of receptor with respect to internal volume [R']
10. Initial rate constant for ion flux.

This work was supported in part by a grant from the National Institute of Neurological and Communicative Disorders and Stroke (DHS 5RO1 NS20377-03). Dr. Subbarao holds a Missouri Institute of Psychiatry Fellowship.

Received for publication 12 June 1987 and in final form 11 July 1988.

REFERENCES

Allan, A. M., R. A. Harris, K. Subbarao, and D. J. Cash. 1985. Demonstration of GABA stimulated $^{36}Cl^-$ flux with isolated brain membranes. *Fed. Proc.* 44:1634.

Aoshima, H., D. J. Cash, and G. P. Hess. 1981. The mechanism of inactivation (desensitization) of the acetylcholine receptor. Investigations by fast reaction techniques with membrane vesicles. *Biochemistry.* 20:3467–3474.

Bauman, A., J. P. Changeux, and P. Benda. 1970. Purification of membrane fragments derived from the nonexcitable surface of the eel electroplax. *FEBS (Fed. Eur. Biochem. Soc.) Lett.* 8:145–148.

Booth, R. F. G., and J. B. Clark. 1978. A rapid method for the preparation of relatively pure metabolically competent synaptosomes from a rat brain. *Biochem. J.* 176:365–370.

Cartaud, J., E. L. Benedetti, M. Kasai, and J.-P. Changeux. 1971. *In vivo* excitation of purified membrane fragments by cholinergic agonists. *J. Membr. Biol.* 6:81–88.

Cartaud, J., E. L. Benedetti, A. Sobel, and J.-P. Changeux. 1978. A morphological study of the cholinergic receptor protein from *Torpedo marmorata* in its membrane environment and in its detergent extracted purified form. *J. Cell Sci.* 29:313–337.

Cash, D. H., H. Aoshima, and G. P. Hess. 1981. Acetylcholine-induced cation translocation across cell membranes and inactivation of the acetylcholine receptor: chemical kinetic measurements in the msec time region. *Proc. Natl. Acad. Sci. USA.* 78:3318–3322.

Cash, D. J., H. Aoshima, E. B. Pasquale, and G. P. Hess. 1985. Acetylcholine-receptor-mediated ion fluxes in *Electrophorus electricus* and *Torpedo californica* membrane vesicles. *Rev. Physiol. Biochem. Pharmacol.* 102:73–117.

Cash, D. J., and G. P. Hess. 1981. Quenched flow technique with plasma membrane vesicles: acetylcholine-receptor-mediated transmembrane ion-flux. *Anal. Biochem.* 112:39–51.

Cash, D. J., and G. P. Hess. 1980. Molecular mechanism of acetylcholine-receptor controlled ion translocation across cell membranes. *Proc. Natl. Acad. Sci. USA.* 77:842–846.

Cash, D. J., and K. Subbarao. 1987*a*. γ-Aminobutyric acid (GABA) mediated transmembrane chloride flux with membrane vesicles from rat brain measured by quench flow technique: kinetic homogeneity of ion-flux and receptor desensitization. *Life Sci.* 41:437–445.

Cash, D. J., and K. Subbarao. 1987*b*. Desensitization of γ-aminobutyric acid receptor from rat brain: two distinguishable receptors on the same membrane. *Biochemistry.* 26:7556–7562.

Cash, D. J., and K. Subbarao. 1987*c*. Two desensitization processes of GABA receptor from rat brain. *FEBS (Fed. Eur. Biochem. Soc.) Lett.* 217:129–133.

Cash, D. J., and K. Subbarao. 1987*d*. Channel opening of γ-aminobutyric acid receptor from rat brain: molecular mechanisms of the receptor responses. *Biochemistry.* 26:7562–7570.

Chasin, M., F. Mamrak, and S. G. Samaniego. 1974. Preparation and properties of a cell-free hormonally responsive adenylate cyclase from guinea pig brain. *J. Neurochem.* 22:1031–1038.

Cotman, C., D. H. Brown, B. W. Harrell, and N. G. Anderson. 1970. Analytical differential centrifugation: an analysis of the sedimentation properties of synaptosomes, mitochondria and lysosomes from rat brain homogenates. *Arch. Biochem. Biophys.* 136:436–447.

Cotman, C. W., and D. A. Mathews. 1971. Synaptic plasma membranes from rat brain synaptosomes: isolation and partial characterization. *Biochim. Biophys. Acta.* 249:380–394.

Daly, J. W., E. McNeal, C. Partington, M. Neuwirth, and C. R. Creveling. 1980. Accumulations of cyclic AMP in adenine-labelled cell-free preparations from guinea pig cerebral cortex: role of γ-adrenergic and H_1-histaminergic receptors. *J. Neurochem.* 35:326–337.

DeRobertis, E., A. P. de Iraldi, G. R. de L. Arnaiz, and L. Salganicoff. 1962. Cholinergic and non-cholinergic nerve endings in rat brain. I. Isolation and subcellular distribution of acetylcholinesterase. *J. Neurochem.* 9:23–35.

Dodd, P. R., J. A. Hardy, A. E. Oakley, J. A. Edwardson, E. K. Penny, and J. P. Delaunoy. 1981. A rapid method for preparing synaptosomes: comparison with alternative procedures. *Brain Res.* 226:107–118.

Fu, J. L., D. B. Donner, D. E. Moore, and G. P. Hess. 1977. Allosteric interactions between the membrane-bound acetylcholine receptor and chemical mediators: equilibrium measurements. *Biochemistry.* 16:678–684.

Gray, E. G., and V. P. Whittaker. 1962. The isolation of nerve endings from brain: an electron-microscopic study of cell fragments derived by homogenization and centrifugation. *J. Anat. (Lond.).* 96:79–88.

Guidotti, G. 1979. Coupling of ion transport to enzyme activity. *In* The Neurosciences. F. O. Schmitt and F. G. Worden, editors. MIT Press, Boston. 831 pp.

Hajos, F. 1975. An improved method for the preparation of synaptosomal fractions in high purity. *Brain Res.* 93:485–489.

Harris, R. A., and A. M. Allan. 1985. Functional coupling of γ-aminobutyric acid receptors to chloride channels in brain membranes. *Science (Wash. DC).* 228:1108–1110.

Hess, G. P., and J. P. Andrews. 1977. Functional acetylcholine receptor electroplax membrane microsacs (vesicles): purification and characterization. *Proc. Natl. Acad. Sci. USA.* 74:482–486.

Hess, G. P., J. P. Andrews, G. E. Struve, and S. E. Coombs. 1975. Acetylcholine-receptor-mediated ion flux in electroplax membrane preparations. *Proc. Natl. Acad. Sci. USA.* 72:4371–4375.

Hess, G. P., H. Aoshima, D. J. Cash, and B. Lenchitz. 1981. The specific reaction rate of acetylcholine-receptor-controlled ion translocation: a comparison of measurements with membrane vesicles and with muscle cells. *Proc. Natl. Acad. Sci. USA.* 78:1361–1365.

Hess, G. P., D. J. Cash, and H. Aoshima. 1983. Acetylcholine receptor-controlled ion translocation: chemical kinetic investigations of the mechanism. *Annu. Rev. Biophys. Bioeng.* 12:443–473.

Hess, G. P., D. J. Cash, and H. Aoshima. 1980. Kinetic mechanism of acetylcholine-receptor controlled ion flux: flow quench kinetic measurements of acetylcholine-induced flux in membrane vesicles. *Neurochem. Int.* 2:233–242.

Hess, G. P., D. J. Cash, and H. Aoshima. 1979. Acetylcholine-receptor-controlled ion fluxes in membrane vesicles investigated by fast reaction techniques. *Nature (Lond.).* 282:329–331.

Hess, G. P., S. Lipkowitz, and G. E. Struve. 1978. Acetylcholine-receptor-mediated ion flux in electroplax membrane microsacs (vesicles): change in mechanism produced by asymmetrical distribution of sodium and potassium ions. *Proc. Natl. Acad. Sci. USA.* 75:1703–1707.

Hess, G. P., E. B. Pasquale, J. W. Walker, and M. G. McNamee. 1982. Comparison of acetylcholine receptor-controlled cation flux in membrane vesicles from *Torpedo californica* and *Electrophorus electricus:* chemical kinetic measurements in the millisecond time region. *Proc. Natl. Acad. Sci. USA.* 79:963–967.

Hollingsworth, E. B., E. T. McNeal, J. L. Burton, R. J. Williams, J. W. Daly, and C. R. Creveling. 1985. Biochemical characterization of a filtered synaptosome preparation for guinea pig cerebral cortex: cyclic adenosine 3':5'-monophosphate-generating systems, receptors and enzymes. *J. Neurosci.* 5:2240–2253.

Horn, A. S., and O. T. Phillipson. 1976. A noradrenaline sensitive adenylate cyclase in rat limbic forebrain: preparation properties and the effects of agonists, adrenolytics and neuroleptic drugs. *Eur. J. Pharmacol.* 37:1–11.

Jeng, A. Y., P. A. St. John, and J. B. Cohen. 1981. Fractionation by velocity sedimentation of *Torpedo* nicotinic post-synaptic membranes. *Biochim. Biophys. Acta.* 646:411–421.

Kaback, H. R. 1970. Transport. *Annu. Rev. Biochem.* 39:561–598.

Kasai, M., and J.-P. Changeux. 1971. *In vitro* excitation of purified membrane fragments by cholinergic agonists. I. Pharmacological properties of the excitable membrane fragments. *J. Membr. Biol.* 6:1–23.

Lehninger, A. L. 1964. The Mitochondrion. Benjamin, New York.

Loescher, W., G. Bohme, F. Muller, and S. Pagliusi. 1985. Improved method for isolating synaptosomes from 11 regions of one rat brain: electron microscopic and biochemical characterization and use in the study of drug effects in nerve terminal γ-aminobutyric acid *in vivo*. *J. Neurochem.* 45:879–889.

Neubing, P. R., and J. B. Cohen. 1980. Permeability control by cholinergic receptors in *Torpedo* postsynaptic membranes: agonist dose-reponse relations measured at second and millisecond times. *Biochemistry.* 19:2770–2779.

Psychoyos, S., J. Dove, B. Stowbridge, and J. Nusynowitz. 1982. Highly activatable adenylate cyclase in [2.^{3}H] adenine-prelabeled vesicles prepared from guinea pig cerebral cortex by a simplified procedure. *J. Neurochem.* 38:1437–1445.

Racker, E. 1970. Membranes of Mitochondria and Chloroplasts. Van Nostrand-Reinhold, New York.

Rosenberg, P., I. Silman, E. Ben-David, A. DeVries, and E. Condrea. 1977. Characterization of membranes obtained from electric organ of the electric eel by sucrose gradient fractionation and by microdissection. *J. Neurochem.* 29:561–578.

Sachs, A. B., B. Lenchitz, R. L. Noble, and G. P. Hess. 1982. A new method for large scale preparation of membrane vesicles which are selectively permeable to specific ions: acetylcholine-receptor-containing vesicles. *Anal. Biochem.* 124:185–190.

Sanchez, G. M., M. C. Toledo, and M. P. Gonzalez. 1984. The chloride channel opening by GABA as an energy dependent process. *Rev. Esp. Fisiol.* 40:375–380.

Schwartz, R. D., P. Skolnick, T. W. Seale, and S. M. Paul. 1986. Demonstration of GABA/barbiturate-receptor-mediated chloride transport in rat brain synaptoneurosomes: a functional assay of GABA receptor-effector coupling. *Adv. Biochem. Pharmacol.* 41:33–49.

Smith, P. K., R. I. Krohn, G. T. Hermanson, A. K. Mallia, F. H. Gartner, M. D. Provenzano, E. K. Fujimoto, N. M. Goeke, B. J. Olson, and D. C. Klenk. 1985. Measurement of protein using bicinchoninic acid. *Anal. Biochem.* 150:76–85.

Stein, W. D. 1986. Transport and Diffusion across Cell Membranes. Academic Press, New York.

Strader, C. B. D., J.-P. Revel, and M. A. Raftery. 1979. Demonstration of the transmembrane nature of acetylcholine receptor by labeling with anti-receptor antibodies. *J. Cell Biol.* 83:499–510.

Subbarao, K., and D. J. Cash. 1985. Functional responses of the γ-aminobutyric acid receptor from brain. *Soc. Neurosci. Abstr.* 11:275.

Sun, G. Y., and A. Y. Sun. 1972. Phospholipids and acyl groups of synaptosomal and myelin membranes isolated from the cerebral cortex of squirrel monkey (*Saimiri Sciureus.*) *Biochim. Biophys. Acta.* 280:306–315.

Walker, J. W., M. G. McNamee, E. B. Pasquale, D. J. Cash, and G. P. Hess. 1981. Acetylcholine receptor inactivation in *Torpedo californica* electroplax membrane vesicles. Detection of two processes in the millisecond and second time regions. *Biochem. Biophys. Res. Commun.* 100:86–90.